Adv. Functional Materials (2009)

Modeling Polymer Dielectrics/Pentacene Interfaces: On the Role of Electrostatic Energy Disorder on Charge Carrier Mobility

N. G. Martinelli[1], M. Savini[2], L. Muccioli[2], Y. Olivier[1], F. Castet[3], C. Zannoni[2], D. Beljonne[1] and J. Cornil[1]

[1]*Laboratory for Chemistry of Novel Materials*
University of Mons-Hainaut,
Place du Parc 20, B-7000 Mons, Belgium

[2]*Dipartimento di Chimica Fisica e Inorganica and INSTM*
Università di Bologna
Viale Risorgimento 4, IT-40136 Bologna, Italy

[3]*Institut des Sciences Moléculaires, UMR CNRS 5255,*
Université de Bordeaux,
351 Cours de la Libération, FR-33405 Talence, France

Abstract

Force-field and quantum-chemical calculations have been combined to model at the atomistic level the packing of pentacene molecules on two polymer dielectric layers (PMMA versus polystyrene – PS) widely used in field-effect transistors and to assess the impact of electrostatic interactions at the interface on the charge mobility values in the pentacene layers, respectively. The results show unambiguously that the electrostatic interactions introduce a significant energetic disorder in the pentacene layer in contact with the polymer chains; a drop in the hole mobility by a factor of 5 is predicted with PS chains while a factor of 60 is obtained for PMMA due to the presence of polar carbonyl groups.

The field of organic electronics has developed tremendously over the last twenty years. [1] The key advantages of organic semiconductors compared to their inorganic equivalents are the versatility of chemical synthesis, the ease of processing (in particular over large areas), and low production costs. Among the numerous applications, organic field-effect transistors (OFETs) are attractive devices planned to be used as building blocks in low cost electronic components. [2-5] The optimization of their performance requires the improvement of the charge transport properties in organic layers which are quantified by the charge carrier mobility value (μ). [6] FETs based on amorphous silicon yield mobilities around 1 $cm^2\ V^{-1}\ s^{-1}$ while intensive research has now led to values as high as 30 $cm^2\ V^{-1}\ s^{-1}$ for organic materials in the best cases. [7]

In spite of good device performance, a complete understanding of charge transport in organic semiconductors at the microscopic level is still lacking. A hopping regime, in which charges jump from molecule to molecule, is typically assumed to describe charge transport in disordered systems where static positional and energetic disorder promotes charge localization over individual molecules. [8] Similarly, recent theoretical studies have also suggested that the charges get strongly localized in highly ordered systems such as molecular crystals due to thermal fluctuations and the resulting dynamic energetic and/or spatial disorder. [9-11] In OFETs, the charges are confined within a few nanometers from the surface of the dielectrics so that transport mostly operates (at low bias) within the first molecular layer. [3, 12] The transport properties, and hence the charge mobility values, are thus expected to be further affected in the conducting channel by:

- (i) the nature of the insulator layer. A significant drop of the mobility by up to one order of magnitude was reported in OFETs based on polytriarylamine chains when replacing low-k polymer dielectrics by polymethylmethacrylate (PMMA). [13] Similar observations were made in the case of pentacene layers. [14, 15] This deterioration of the mobility was attributed to an increase in the energetic disorder promoted by the polar carbonyl bonds of the PMMA chains. [13] This model is consistent with previous theoretical studies of charge transport in solids formed by molecules bearing a permanent dipole moment. [16] Shifts of the threshold voltages in OFETs upon different surface treatment of the gate insulator have also been

explained on the same basis. [17, 18] In the case of highly polarizable dielectric layers, the formation of Frölich polarons has been suggested, implying that the migration of the charges is slowed down by the nuclear polarization of the dielectric layer; [19] however, this model does not appear to be applicable for polymer dielectrics. [20, 21]

- (ii) the morphology of the organic layer. The formation of grain boundaries is one of the major structural limitations to high charge mobility values. [5, 22, 23] Recent studies on OFETs based on pentacene show that the grain size varies as a function of the nature of the polymer dielectrics and that the carrier mobility is very sensitive to the grain size below a root-mean-square value of about 0.8 μm. [14, 24] The viscoelasticity of the polymer chains, and hence the deposition temperature as well as the deposition rate, may also influence the charge mobility. [14, 25]
- (iii) the nature of the electronic states at the surface. Organic semiconductors typically display a p-type behavior when using SiO_2 as the dielectric layer in FETs due to the presence of electron traps on the surface. [15, 26] These chemical traps can be eliminated by using polymer dielectrics [26] or by treatment of the SiO_2 surface. [15, 27] Correlations between cleaning techniques and OFET electrical characteristics have been clearly established. [28]

Since many parameters are likely to modulate the transport properties in OFET experiments and since the impact of a given factor is generally difficult to extract from experimental measurements, theoretical calculations can prove very useful by shedding light on these effects, as illustrated by recent phenomenological models addressing the role of electrostatic interactions between the semiconducting and dielectric layers. [20] However, studies involving an atomistic description of the system [29, 30] have not been reported so far to the best of our knowledge. Accordingly, we have combined in the present work Molecular Dynamics simulations to establish the organization at the atomistic scale of pentacene molecules on polymer dielectrics and quantum-chemical calculations to assess the actual impact of electrostatic interactions on the charge mobility values.

We focus here on pentacene molecules (*i.e.*, one of the most studied and efficient organic semiconductors) deposited on top of polystyrene (PS) versus PMMA chains, widely used as polymer dielectrics. This choice is motivated by the fact that

PS is non-polar while PMMA features polar bonds associated to the carbonyl groups; moreover, the performance of OFETs involving these interfaces have been assessed [14, 15]

In a way similar to the experimental fabrication of an OFET, [31] we obtained with atomistic molecular dynamics simulations 3D periodic cells consisting of a polymer (PS or PMMA)/pentacene wafer equilibrated at 300 K (see Theoretical methodology). Each slab is about 60 Å thick, allowing for the generation of two independent dielectrics/pentacene interfaces, with the organic semiconductor forming four crystalline layers homeotropically oriented (Figure 1). Note that the finite size of the supercell (60 x 60 Å) does not allow us to describe morphological defects such as grain boundaries.

In order to characterize the impact of energetic disorder in the different pentacene layers on the charge transport properties, we have defined the parameter ΔE_{ij} associated to a charge hopping process as:

$$\Delta E_{ij} = E_i^0 + E_j^+ - (E_i^+ + E_j^0) \quad (1)$$

with E the electrostatic interaction between a pentacene molecule and the PMMA or PS chains. The Coulomb energies were calculated from atomic point charges obtained with density functional theory (DFT) calculations at the B3LYP//aug-cc-pVDZ level and interatomic distances within the minimum image convention; [32] i and j represent the initial and final sites involved in the charge transfer, respectively while 0 [+] denotes a neutral [positively charged] molecule. Note that: (i) we do not account for the possible slight energetic disorder induced by the interactions between the pentacene molecules since our primary focus is to determine the way the charge transport properties are affected by the introduction of the dielectric layer; (ii) electronic polarization effects are found to be limited due to the low polarizability of the saturated polymer chains in the dielectric layer, as supported by additional quantum-chemical calculations (see Figures S1 and S2 in the Supporting information); and (iii) since the Coulomb forces are dominated by the interactions between a pentacene molecule and the nearest repeat units of the polymer chains due to the amorphous nature of the dielectric layer, [20] the use of a macroscopic

dielectric constant is not appropriate at such short distances and has therefore been omitted when calculating the ΔE parameters. [33]

Figure 2 displays the distribution of ΔE_{ij} for all pairs of pentacene molecules in the different layers on top of PMMA *versus* PS, as averaged over 100 snapshots extracted every 100 ps from a MD run of 10 ns; the averaging procedure is justified by the fast lattice dynamics yielding a fast saturation of the width of energetic disorder, as illustrated in Figure S4 of the Supporting information. The distributions are symmetric with respect to zero since each molecule is considered at the same time as a possible initial or final site; all distributions can be fitted with a Gaussian distribution. For each polymer dielectrics, the broadening is the most pronounced in the layer in direct contact with the polymer chains. The evolution of the standard deviation σ of the Gaussian distribution as a function of the distance z from the interface can be fitted by a 1/z function (see Figure S3 of Supporting information), as expected from Coulomb laws. When comparing the two polymers, the main difference is observed in the surface layer where $\sigma_{PMMA} \sim 2\sigma_{PS}$. From a simple qualitative reasoning, we thus expect that the charge transport properties within the pentacene surface layer (*i.e.*, in contact with the polymer) should be significantly affected, with a lower mobility predicted for PMMA.

Next, the impact of the polymer dielectrics on transport properties has been assessed quantitatively by propagating charge carriers within a hopping regime in the different pentacene layers by means of Monte-Carlo simulations, with an explicit account of the electrostatic interactions between the pentacene molecules and the polymer chains (see Theoretical methodology). The use of a hopping model is validated by the fact that OFETs typically operate at room temperature or higher, *i.e.*, in conditions where thermal disorder favors charge localization; [9] the latter is further reinforced by the energetic disorder created by the electrostatic interactions. We emphasize that we are primarily interested here by the changes in the mobility values induced by the presence of the dielectric layer rather than by the absolute values of the mobility, which are dictated by the amplitude of the molecular parameters employed. Figure 3 shows the polar plot of the mobility values obtained for the different pentacene layers (with the charge constrained to remain in the same

layer) in presence of PMMA *versus* PS chains. These plots are generated by rotating the direction of the external electric field (with a typical amplitude of 10^4 V/cm) within the layer in order to explore the anisotropy of charge transport. For each polar angle, the mobility has been calculated for 100 different layer geometries (by extracting a configuration every 100 ps of a total MD run of 10 ns) before getting averaged; the same time-averaged values of ΔE_{ij} have been used in all simulations. The trends observed for the mobility reflect the distributions obtained for the ΔE values. For layers 2 to 4, the influence of the dielectrics on the mobility values is very small, as supported by the narrow energetic distributions. On the contrary, the mobility is significantly lowered in the surface layer (1) due to the increased energetic disorder. We stress that similar mobility values are obtained for the isolated surface layer and for bulk pentacene, thus demonstrating that the drop in the mobility cannot be attributed to changes in the molecular packing at the interface. The mobility is found to be reduced by a factor of 60 for PMMA and 5 for PS compared to bulk pentacene. The calculated ratio of 12 between PMMA and PS is larger than the reported experimental values on the order of 4. [15, 14] However, it is worth recalling that our simulations do not take into account any macroscopic morphological defects such as grain boundaries which are likely to affect the experiment measurements; it has been shown for instance that using PS chains of different molecular weight yields various grain sizes and different mobility values. [14] Similar mobility values are found for PS and PMMA when propagating a hole in the surface layer of the second interface generated with the periodic boundary conditions.

In summary, we have combined classical and quantum-chemical calculations to model at the atomistic level the interface between pentacene layers and a dielectric layer made of either PMMA or PS chains, in relation to their use in OFETs. Our calculations demonstrate univocally that the polarity of the polymer chains increases the amount of energetic disorder in the organic semiconducting layer. However, this effect is only pronounced within the surface layer and rapidly decays in the subsequent layers. These findings indicate that the choice of the chemical nature of polymer dielectrics is critical for the optimization of charge transport properties in OFETs.

Theoretical methodology

Parameterization of the force field

In order to obtain the atomic charges required to describe properly the electrostatic properties of the polymers, we first optimized isotactic quater-styrene and quater-methylmethacrylate at the semi-empirical Hartree-Fock AM1 (Austin Model 1) level using Gaussian03. [34] We have then computed the electrostatic potential fitting charges (ESP [35]) at the density functional theory – DFT – level (using the B3LYP functional and the aug-cc-pVDZ basis set) with the option Dipole (so that the charges also reproduce the dipole moment of the molecule). Charges of all constituting monomers were further averaged and slightly varied in order to have a zero total charge per monomer and a zero charge on the terminal hydrogen atoms. At the B3LYP/aug-cc-pVDZ level, the permanent dipoles of the monomer are estimated to be 4.6 D and 4.3 D for MMA and 0.4 D and 0.2 D for styrene in the saturated (with a C=C double bond) and unsaturated forms (with C-C single bond and valences saturated with two hydrogen atoms), respectively. The pentacene charges were calculated at the same DFT level starting from the X-ray crystalline geometry downloaded from the Cambridge Crystallographic Data Centre; charges were subsequently symmetrised according to the point group of the molecule. The resulting atomic charges were plugged into the AMBER94 molecular mechanics force field [36] used in all MD simulations.

Packing of the polymer chains

Monomers of PMMA and PS in the reacted form (without terminal hydrogens) were first connected to obtain 50 monomer-long linear isotactic chains (Molecular weight: M_{PMMA}=5007.7 g/mol, M_{PS}=5209.2 g/mol). Each chain was replicated 27 times in a cubic lattice to give a starting simulation box with a low density (20304 atoms for PMMA, 21654 atoms for PS). The boxes were first equilibrated at 500 K (*i.e.*, well above the glass transition temperature and close to the melting point); this generates a box size of about 65 Å, then used as input configurations for further runs at progressively lower temperatures until room temperature is reached (300 K) by steps of 25 K. All simulations were done with the Orac molecular dynamics (MD)

program [37] in the isothermal-isobaric (NPT) ensemble at atmospheric pressure, with velocity scaling thermostat, isotropic box changes [38] and 3D periodic boundary conditions (PBC). A maximum integration time step of 10 femtoseconds was used in a multiple time step scheme, [37] for a total equilibration time of at least 10 nanoseconds for each temperature. Long-range electrostatic interactions were dealt with the smooth particle mesh Ewald technique [39] with a 40x40x40 mesh.

Packing of pentacene molecules

A crystalline pentacene sample was built by replicating the experimental crystal unit cell (Z=2) 10x8x2 times in the x,y,z directions to give a total number of 320 molecules. The number of replica in the xy plane was chosen according to the "vapour" or "H" polymorph cell parameters [40] in order to obtain a layer of approximately the same dimension as the polymer box. The initial configuration was submitted to a MD run of 5 nanoseconds at room temperature, atmospheric pressure and by imposing an orthorhombic cell. [38] This simulation demonstrates that the crystalline structure is well preserved at room temperature and is similar to the experimental and theoretically predicted [41] unit cell (see Table 1); the adopted force field is thus adequate in this context.

Sample preparation

In a second stage, four equilibrated pentacene layers were added on top of PMMA and PS samples at T=300 K. To do so, bulk samples with 3D periodic boundary conditions (PBC) were transformed into 2D samples by artificially enlarging the polymer box by 100 Å in the z direction in order to generate two vacuum/polymer interfaces. These samples were equilibrated for about 1 nanosecond at constant volume to let dangling chains collapse on the surface before the insertion of pentacene in the box. 3D PBC were then restored so as to generate two independent polymer dielectrics/pentacene interfaces. Afterwards, a pressure of 100 atmospheres was imposed to speed-up the compression in further MD simulations in the NPT ensemble with a triclinic cell for pentacene. [38] As soon as the pentacene/polymer interface appeared to be sufficiently smooth, the pressure was restored to one atmosphere and equilibration and production runs were performed at 300K during 10

ns to produce the morphologies required for the charge transport simulations, see Figure 1.

Charge mobility values

The transfer rate k_{if} between the initial (*i*) and final (*f*) sites has been estimated in the framework of the standard Marcus-Levich-Jortner theory as [42]:

$$k_{if} = \frac{2\pi}{\hbar} V_{if}^2 \frac{1}{\sqrt{4\pi\lambda_s k_B T}} \sum_{n=0}^{\infty} \exp(-S) \frac{S^n}{n!} \times \exp\left[-\frac{(\Delta G^0 + \lambda_s + n\hbar\omega)^2}{4\lambda_s k_B T} \right] \qquad (2)$$

with k_B the Boltzmann constant and T the temperature. V_{if} is the transfer integral between the HOMO levels of the two interacting molecules, calculated here in a direct way at the semi-empirical Hartree Fock INDO (Intermediate Neglect of Differential Overlap) level, as detailed in Ref. [43]. For all snapshots, the transfer integrals have been calculated for all pairs of adjacent molecules in a given layer (the values are vanishingly small for molecules located in different, even adjacent layers). S is the Huang-Rhys factor defined as $S=\lambda_i/\hbar\omega$, with λ_i the internal reorganization energy and $\hbar\omega$ the energy of an effective mode assisting the charge transfer (and n the vibrational quantum number). λ_i has been estimated in a previous study to be 97 meV for holes in pentacene [44] and $\hbar\omega$ set equal here to 0.2 eV (*i.e.*, the typical energy for C-C bond stretching or aromatic ring breathing modes) so that S = 0.485. λ_s is the external reorganization energy set equal to a reasonable value of 0.2 eV in both cases. [46] We stress that the choice of these values is not critical since it does not affect significantly the ratio of the mobility in the presence of the different dielectric layers which modulates the $\Delta G°$ parameter. The latter is expressed as:

$$\Delta G^0 = e \cdot \vec{F} \cdot \vec{d} + \Delta E_{ij} \qquad (3)$$

with the first term reflecting the application of an external electric field [45] and the second the amount of energetic disorder. The ΔE_{ij} values have been averaged over the time characteristic of a jump (on the order of a few picoseconds) and were found to be very similar to those reported in Figure 2 over the whole dynamics (see Supplementary Information). Interestingly, without averaging, the mobility values are vanishingly small due to the formation of deep trap levels. In a second stage, the transfer rates have been injected into a Monte-Carlo scheme to propagate a single charge in the various pentacene layers following a procedure detailed in Ref. [45]. If d

is the total distance traveled by the charge, τ the total time obtained from the inverse of the rates of all accepted jumps and F the amplitude of the applied electric field (a typical value of 10^4 V/cm is used in our simulations), the mobility μ is ultimately obtained as:

$$\mu = d/(\tau F) \tag{4}$$

Acknowledgements

We acknowledge stimulating discussions with Prof. Paul Heremans (IMEC). The work in Mons is partly supported by the Belgian Federal Governement "Interuniversity Attraction Pole in Supramolecular Chemistry and Catalysis, PAI 5/3"; the European projects MODECOM (NMP3-CT-2006-016434; the European Community's Seventh Framework Programme (*FP7/2007-2013*) under grant agreement 212311; and the Belgian National Fund for Scientific Research (FNRS/FRFC). J.C. and D.B. are FNRS Research Fellows; N.M. acknowledges a grant from the « Fonds pour la Formation à la Recherche dans l'Industrie et dans l'Agriculture (FRIA) ». The work in Bologna is partly supported by the European project MODECOM (NMP3-CT-2006-016434) and by the Emilia-Romagna regional project PRITT "NANOFABER".

Figures

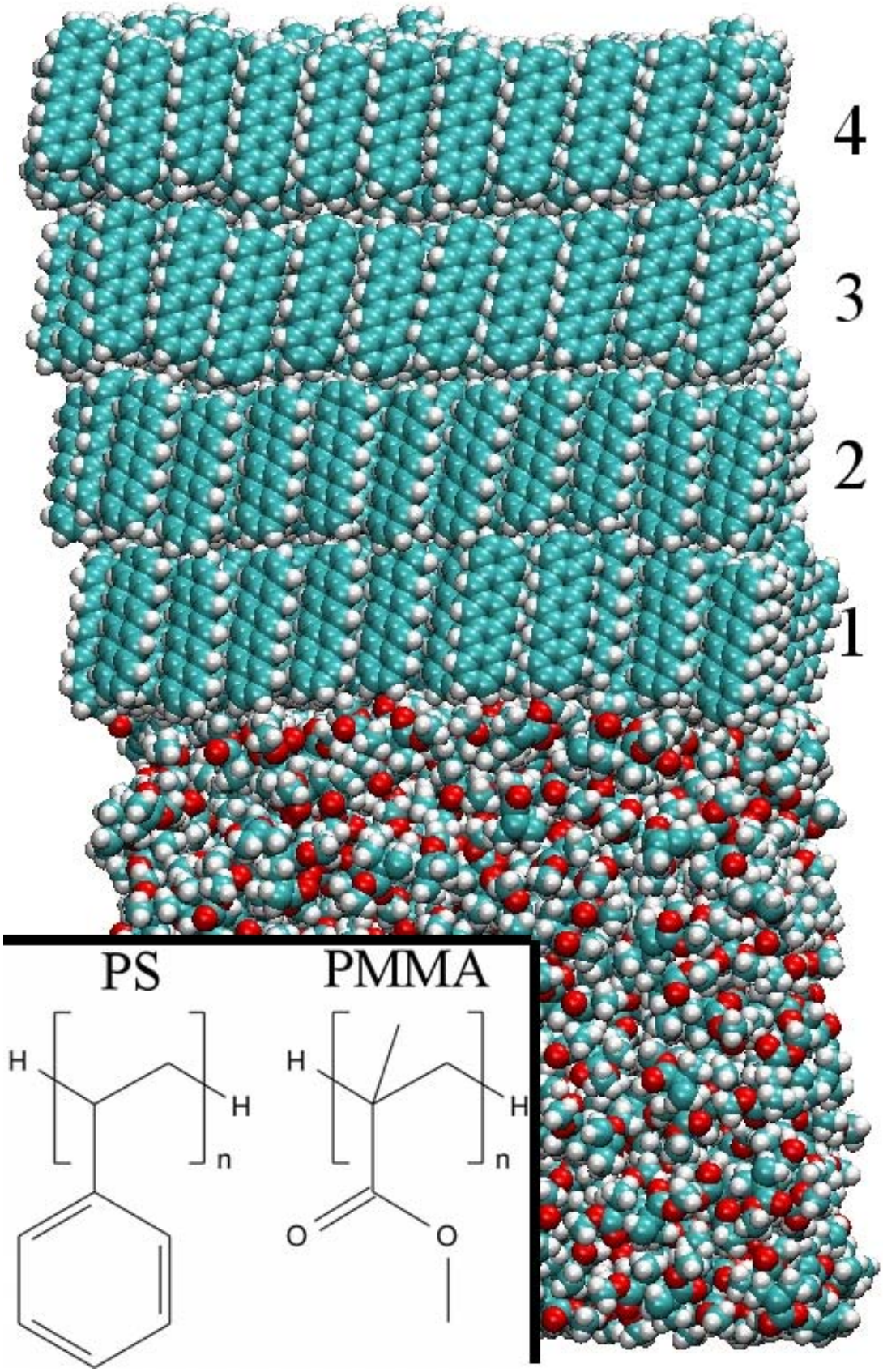

Figure 1

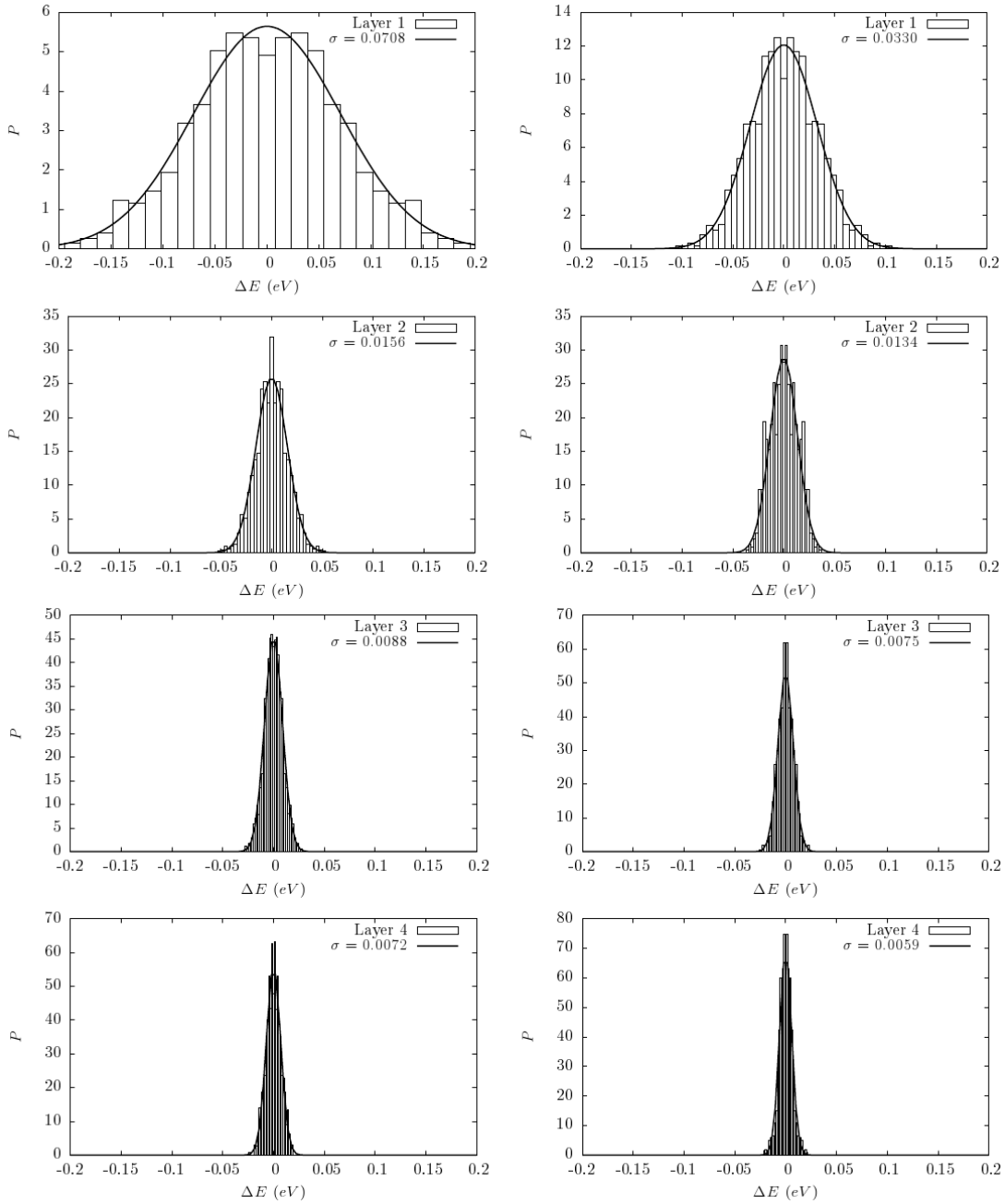
Layer 1
σ = 0.0708
Layer 1
σ = 0.0330
Layer 2
σ = 0.0156
Layer 2
σ = 0.0134
Layer 3
σ = 0.0088
Layer 3
σ = 0.0075
Layer 4
σ = 0.0072
Layer 4
σ = 0.0059
P
ΔE (eV)

Figure 2

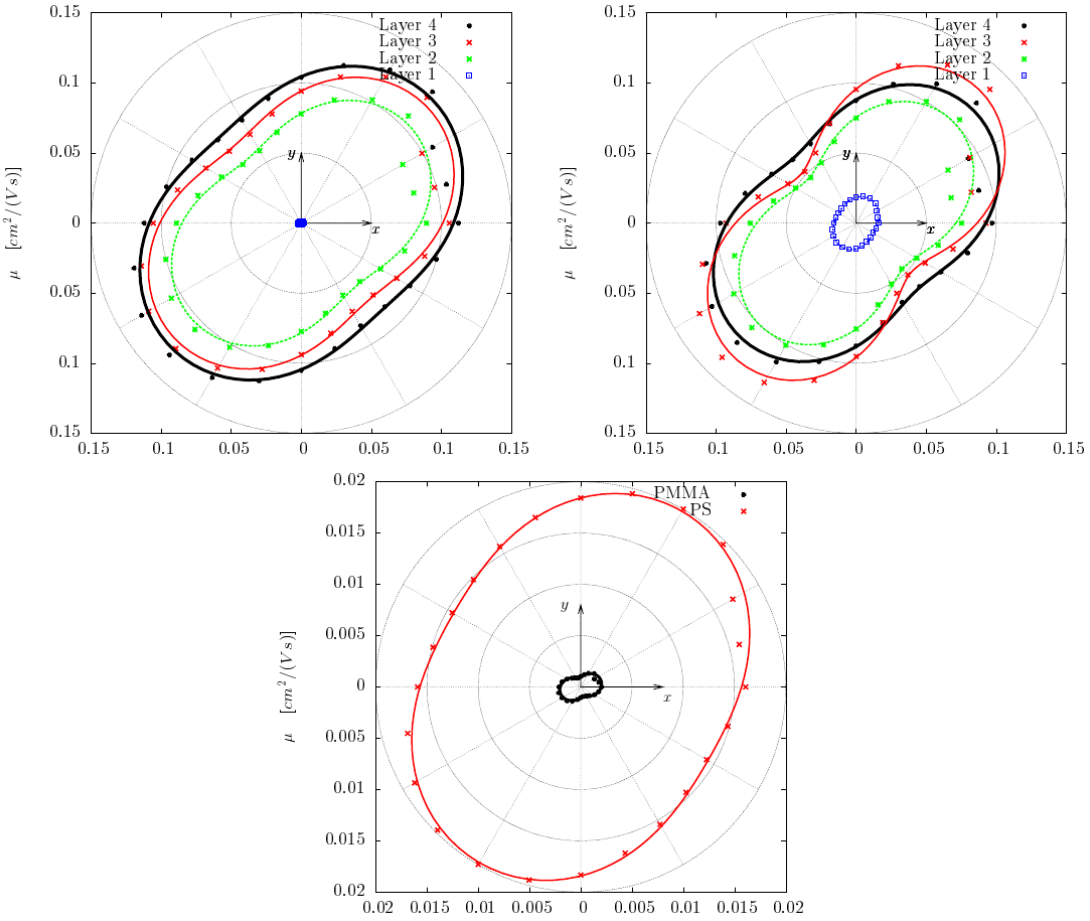

Figure 3

PENTACENE	Ref. [40]	Simulation	Ref. [41]
density (g/cm3)	1.35	1.334	1.36
a (Å)	6.265	6.29	5.986
b (Å)	7.786	7.81	7.776
c (Å)	14.511	14.6	14.949
α (deg)	76.65	76.65	79.45
β (deg)	87.50	87.50	84.17
γ (deg)	84.61	84.61	85.71
T (K)	293	298	293

Table 1

Captions

Figure 1: Atomistic description of the pentacene/polymethylmethacrylate dielectrics interface. The inset shows the chemical structures of the two polymers dielectrics studied.

Figure 2: Distribution of the site energy difference ΔE_{ij} in the four pentacene layers in presence of PMMA (left) and PS (right). A fit with a Gaussian distribution is done in each case (the corresponding standard deviation is given). The labeling of the layers is given in Figure 1.

Figure 3: Polar plots of the mobility calculated for the four pentacene layers in presence of PMMA (top left) and PS (top right); zoom on layer 1 for both polymers (bottom). In each plot, the radius corresponds to the mobility value and the angle to the electric field orientation.

Table 1: Comparison of the unit cell properties for the H polymorph of pentacene: experimental X-ray values, [40] results from the present MD simulations based on $10\times8\times2$ replicas of the experimental unit cell, [40] theoretical predictions by quasi-harmonic lattice dynamics simulations. [41]

References

[1] Handbook of Conducting Polymers, 3rd Edition", edited by T.A. Skotheim and J.R. Reynolds (CRC Press, Boca Raton, 2007)
[2] D. Braga, G. Horowitz, *Adv. Mater.* **2009**, *21*, 1
[3] S. Allard, M. Forster, B. Souharce, H. Thiem, U. Scherf, *Angew. Chem. Int. Edit.* **2008**, *47*, 4070
[4] J. Zaumseil, H. Sirringhaus, *Chem. Rev.* **2007**, *107*, 1296
[5] G. Horowitz, *Adv. Mater.* **1998**, *10*, 365
[6] V. Coropceanu, J. Cornil, D.A. da Silva Filho, Y. Olivier, R. Silbey, J.L. Brédas, *Chem. Rev.* **2007**, *107*, 926
[7] V. Podzorov, E. Menard, A. Borissov, V. Kiryukhin, J.A. Rogers, M.E. Gershenson, *Phys. Rev. Lett.* **2004**, *93*, 086602
[8] H. Bässler, *Phys. Status Solidi B* **1993**, *175*, 15
[9] A. Troisi, *Adv. Mater.* **2007**, *19*, 2000
[10] A. Troisi, G. Orlandi, *J. Phys. Chem. A* **2006**, *110*, 4065
[11] A. Troisi, G. Orlandi, J.E. Anthony, *Chem. Mater.* **2005**, *17*, 5024
[12] F. Dinelli F, M. Murgia, P. Levy, M. Cavallini, F. Biscarini, D. M. de Leeuw, *Phys. Rev. Lett.* **2004**, *92,* 116802
[13] J. Veres, S.D. Ogier, W. Leeming, D.C. Cupertino, S.M. Khaffaf, *Adv. Funct. Mater.* **2003**, *13*, 199
[14] C. Kim, A. Facchetti, T.J. Marks, *Science* **2007**, *318*, 76
[15] N. Benson, C. Melzer, R. Schmechel, H. von Seggern, *Phys. Status Solidi A* **2008**, *205*, 475
[16] P.M. Borsenberger, J.J. Fitzgerald, *J. Phys. Chem.* **1993**, *97*, 4815
[17] K.P. Pernstich, C. Glodmann, C. Krellner, D. Oberhoff, D.J. Gundlach, B. Batlogg, *Synth. Met.* **2004**, *146*, 325
[18] J. Takeya, T. Nishikawa, T. Takenobu, S. Kobayashi, Y. Iwasa, T. Mitani, C. Goldmann, C. Krellner, B. Batlogg, *Appl. Phys. Lett.* **2004**, *85*, 5078
[19] I.N. Hulea, S. Fratini, H. Xie, C.L. Mulder, N.N. Iossad, G. Rastelli, S. Ciuchi, A.F. Morpurgo, *Nat. Mater.* **2006**, *5*, 982
[20] T. Richards, M. Bird, H. Sirringhaus, *J. Chem. Phys.* **2008**, *128*, 234905
[21] J.F. Chang, H. Sirringhaus, M. Giles, M. Heeney, I. McCulloch, *Phys. Rev. B* **2007**, *76*, 205204
[22] S. Verlaak, P. Heremans, *Phys. Rev. B* **2007**, *75*, 115127
[23] D.H. Kim, H.S. Lee, H. Yang, L. Yang, K. Cho, *Adv. Funct. Mater.* **2008**, *18*, 1363
[24] C. Kim, A. Facchetti, T.J. Marks, *Adv. Mater.* **2007**, *19*, 2561
[25] A. Gerlach, S. Sellner, S. Kowarik, F. Schreiber, *Phys. Status Solidi A* **2008**, *205*, 461
[26] L.L. Chua, J. Zaumseil, J.F. Chang, E.C.W. Ou, P.K.H. Ho, H. Sirringhaus, R.H. Friend, *Nature* **2005**, *434*, 194
[27] M.H. Yoon, A. Facchetti, T.J. Marks, *P. Natl. Acad. Sci. USA* **2005**, *102*, 4678
[28] F. Todescato, R. Capelli, F. Dinelli, M. Murgia, N. Camaioni, M. Yang, R. Bozio, M. Muccini, *J. Phys. Chem. B* **2008**, *112*, 10130
[29] R. Berardi, L. Muccioli, C. Zannoni, *ChemPhysChem* **2004**, *5*, 104
[30] G. Tiberio, L. Muccioli, R. Berardi, C. Zannoni, *ChemPhysChem* **2009**, *10*, 125
[31] M. E. Gershenson, V. Podzorov, A. F. Morpurgo, *Rev. Mod. Phys.* **2006**, *78*, 973
[32] M. P. Allen, D. J. Tildesley, in *Computer Simulations of Liquids*, Oxford University Press, UK **1987**.

[33] C. Curutchet, G. D. Scholes, B. Mennucci, R. Cammi, *J. Phys. Chem. B* **2007**, *111*, 13253
[34] M.J. Frisch *et al.* Gaussian 03. Gaussian, Inc., Wallingford, CT, 2004
[35] B.H. Besler, K.M. Merz, P.A. Kollman, *J. Comput. Chem.* **1990**, *11*, 431
[36] W.D. Cornell, P. Cieplak, C.I. Bayly, I.R. Gould, K.M. Merz, Ferguson D.M., D.C. Spellmeyer, T. Fox, J.W. Caldwell, P.A. Kollman, *J. Am. Chem. Soc.* **1995**, *117*, 5179
[37] P. Procacci, T.A. Darden, E. Paci, M. Marchi, *J. Comput. Chem.* **1997**, *18*, 1848
[38] M. Parrinello, A. Rahman, *J. Appl. Phys.* **1981**, *51*, 7182
[39] U. Essmann, L. Perera, M.L. Berkowitz , T. Darden, H. Lee, L.G. Pedersen, *J. Chem. Phys.* **1995**, *103*, 8577
[40] T. Siegrist, C. Kloc, J.H. Schon, B. Batlogg, R.C. Haddon, S. Berg, G.A. Thomas, *Angew. Chem. Int. Edit.* **2001**, *40*, 1732
[41] R. G. Della Valle, E. Venuti, L. Farina, A. Brillante, *J. Phys. Chem. A* **2004**, *108*, 1822
[42] J. Jortner, *J. Chem. Phys.* **1976**, *64*, 4860
[43] A. Van Vooren, V. Lemaur, A.J. Ye, D. Beljonne, J. Cornil, *ChemPhysChem* **2007**, *8*, 1240
[44] V. Coropceanu, M. Malagoli, D.A. da Silva Filho, N.E. Gruhn, T.G. Bill, J.L. Brédas, *Phys. Rev. Lett.* **2002**, *89*, 275503
[45] Y. Olivier, V. Lemaur, J.L. Brédas, J. Cornil, *J. Phys. Chem. A* **2006**, *110*, 6356
[46] V. Lemaur, M. Steel, D. Beljonne, J.L. Brédas, J. Cornil, *J. Am. Chem. Soc.* **2005**, *127*, 6077

Supporting information

Modeling Polymer Dielectrics/Pentacene Interfaces: On the Role of Electrostatic Energy Disorder on Charge Carrier Mobility

N. G. Martinelli, M. Savini, F. Castet, L. Muccioli, Y. Olivier, F. Castet, C. Zannoni, D. Beljonne and J. Cornil

Polarization versus Electrostatic Effects

The impact of polarization effects on the energetic disorder has been estimated using a mixed Valence-Bond/Hartree-Fock (VB/HF) approach detailed in Ref. [S1] This approach is based on the semi-empirical Hartree-Fock Austin Model 1 (AM1) method and involves fragment orbitals that can be relaxed in a controlled way. The extent of polarization effects can be assessed by comparing the magnitude of the Coulomb interactions at the interface with and without electronic relaxation effects.

We have made this comparison in the case of polystyrene where we expect the largest polarization effects due to the presence of polarizable benzene units. To do so, a snapshot of the pentacene/polystyrene interface has been modified to retain only the benzene rings in the dielectric layer due to computational limits. The system subjected to the quantum-chemical approach is finally made of a single pentacene molecule (neutral or charged) on top of the benzene units within a distance of 20 Å (Figure S1); similar results were obtained for larger cut-off distances. The ΔE distribution has been calculated with Eq. 1 by considering all pairs of adjacent pentacene molecules in layer 1. The resulting distributions shown in Figure S2 demonstrate that the difference between the non-relaxed and relaxed systems is small and hence that the impact of 'dynamic' polarization effects is weak.

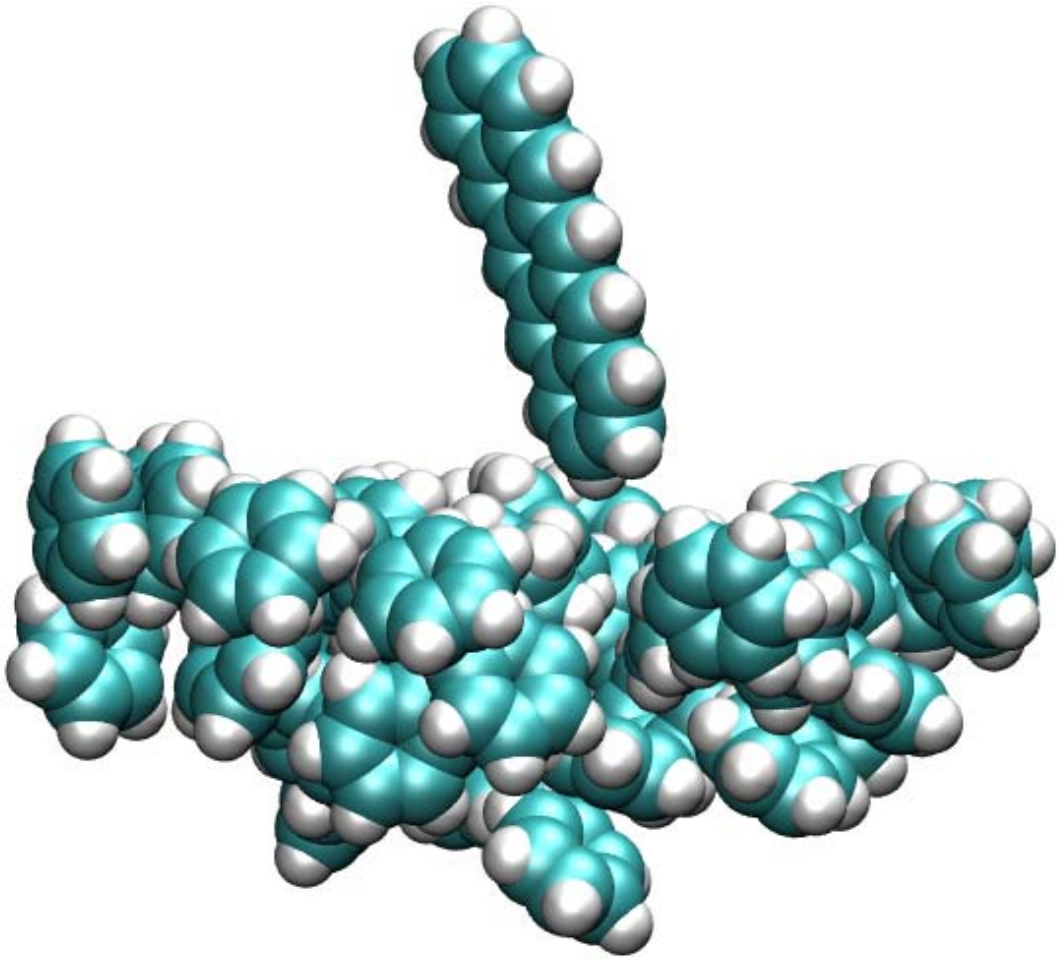

Figure S1: Model pentacene/polystyrene interface where each monomer unit has been replaced by a benzene molecule.

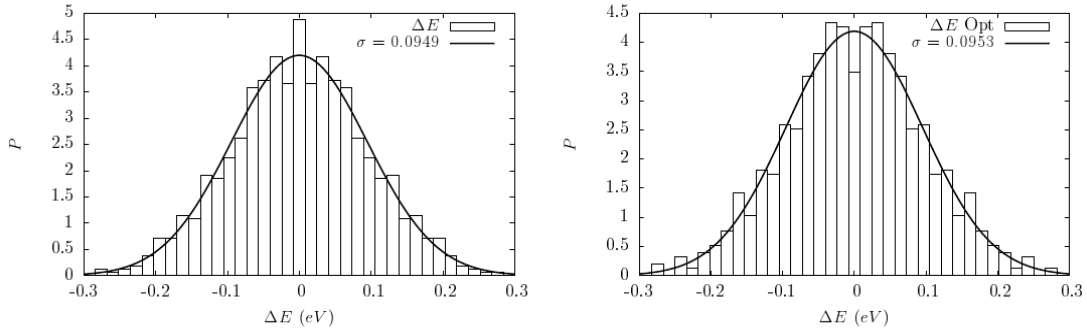

Figure S2: Distribution of ΔE_{ij} in a layer of pentacenes on top of polarisable benzene units for non-relaxed (left) and relaxed (right) molecular orbitals.

Width of the energetic disorder in the different layers

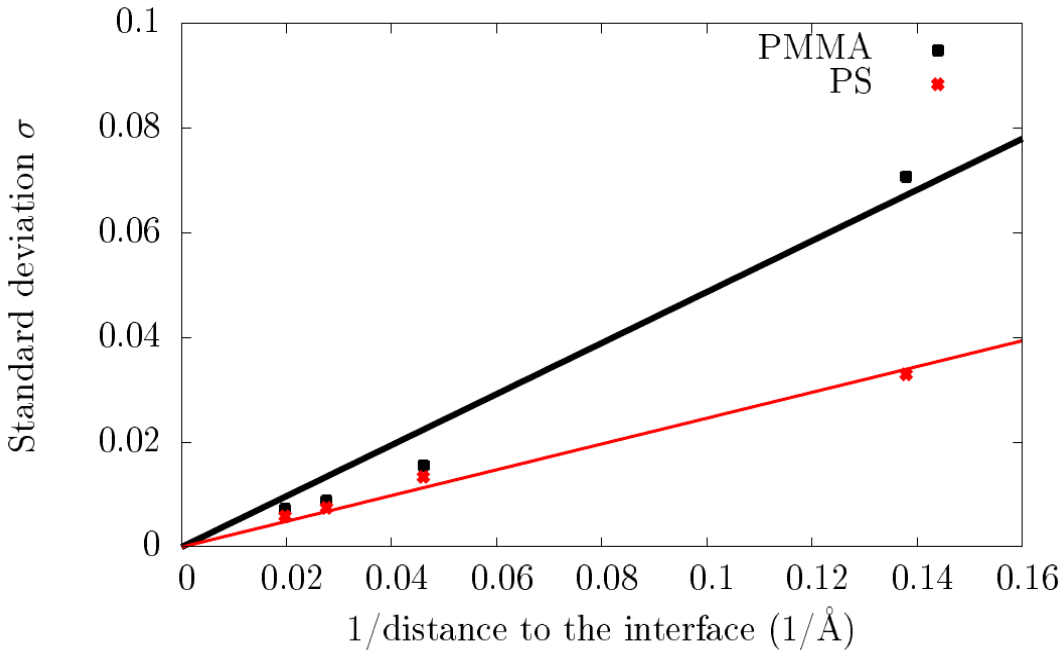

Figure S3: Evolution of the broadening parameter σ in the different pentacene layers in the presence of the PMMA *versus* PS chains. The function y = ax is used for fitting the data; a_{PS} = 0.25 and a_{PMMA} = 0.49.

Time evolution of the broadening parameter

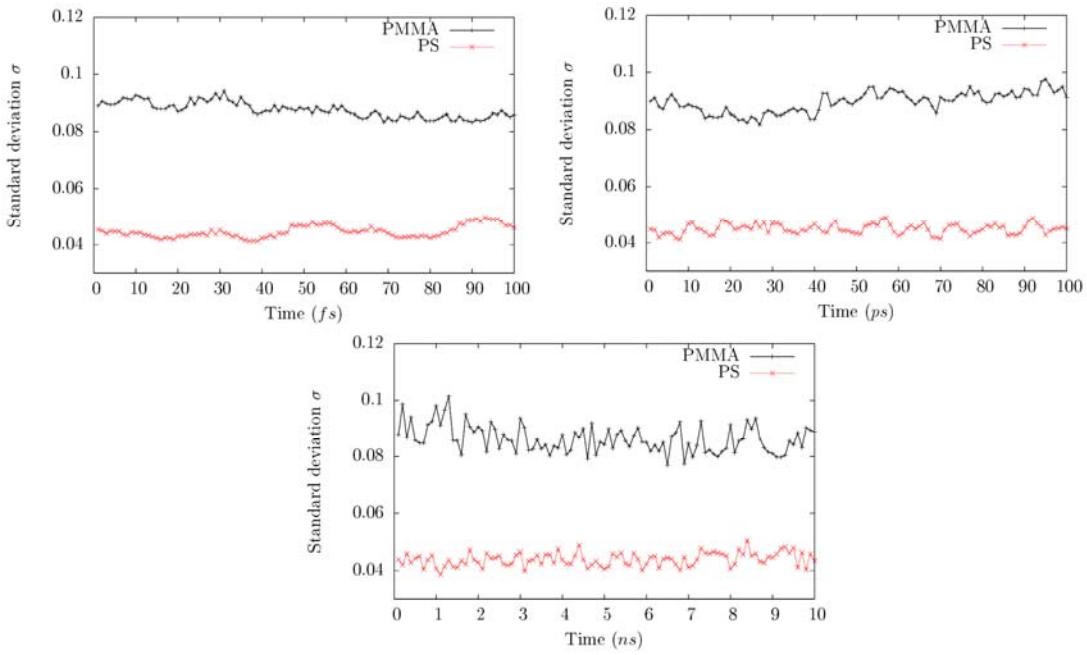

Figure S4: Time evolution of the broadening parameter σ in the first layer of pentacene in presence of PMMA *versus* PS chains. ΔE_{ij} is calculated using instantaneous values of energies.

References

[S1] F. Castet, P. Aurel, A. Fritsch, L. Ducasse, D. Liotard, M. Linares, J. Cornil, D. Beljonne, *Phys. Rev. B.* **2008**, *77*, 115210